PROCEEDINGS OF SCIENCE

Probing EFT in canonical and associated top quark production

Robert Schöfbeck[a,*]

[a] *Institute of High Energy Physics of the Austrian Academy of Sciences (HEPHY)*

E-mail: robert.schoefbeck@oeaw.ac.at

Processes involving the top quark can probe phenomena beyond the standard model (SM) in different ways. The SM Effective Field Theory framework (SM-EFT) allows a model-independent parametrization of deviations from the SM, thereby coping with the large variety of potential fundamental models. The CMS Collaboration is pioneering EFT measurements and moves towards exploiting the full potential of the data in the most global way possible. This contribution covers various analysis strategies for constraining top quark SM-EFT couplings.

**** The European Physical Society Conference on High Energy Physics (EPS-HEP2021), ****
**** 26-30 July 2021 ****
**** Online conference, jointly organized by Universität Hamburg and the research center DESY ****

[*] Speaker

PoS(EPS-HEP2021)490

1. Introduction

With no clear sign of phenomena beyond the standard model (BSM) at the TeV energy scale from the LHC experiments, analyses with top quarks and Higgs bosons enter the precision regime. Parametrizing the theoretical landscape of fundamental BSM models with an effective field theory (EFT) [1–5] turns this wealth of experimental data into sensitive probes of generic symmetry-preserving modifications of the standard model (SM). In particular, the differential cross section measurements of canonical top quark production and top quark pair production in association with an SM boson test the coupling structure of third-generation quarks. I review three top-quark measurements by the CMS Collaboration[6–8] with interpretations in the SM-EFT context in this contribution. Each puts a different emphasis on the number of simultaneously varied Wilson coefficients (WCs), the model parameters that control the strength of the SM-EFT operators responsible for the BSM deviations. The modified interactions enter the production and the decay processes of SM particles, and relations imposed by the SM gauge symmetry account for a complex interplay of effects in the various final states.

2. Experimental results

A search for top quarks produced in association with additional leptons [6] uses a data set of 41.5 fb^{-1} taken during 2017. It tests 16 Wilson coefficients in two broad groups. Operators with top quarks and a Higgs boson, a W boson, a Z boson, or a photon (γ) affect the production rates of $\mathrm{t\bar{t}}$ pairs in association with extra bosons. Four-fermion operators, in turn, affect the $\mathrm{t\bar{t}}\ell\bar{\ell}$ and $\mathrm{t\bar{t}}\ell\nu$ final states with an additional lepton pair off the mass shell. The search is conducted simultaneously in 35 signal regions, defined in lepton multiplicity, the charge of the leptons, and jet- and b-tag multiplicities. A profile-likelihood test statistic is used to constrain nuisances related to systematic uncertainties in various experimental effects. Figure 1 (left) shows prediction and observation for various search bins defined in lepton multiplicity and lepton charge after the likelihood fit. No significant deviation from the SM expectation is observed. In Figure 1 (right), confidence contours in the two-dimensional plane spanned by the Wilson coefficients $c_{\varphi\mathrm{t}}$ and $c_{\mathrm{t}\varphi}$ are shown. These operators are responsible for modifications of the $\mathrm{t\bar{t}Z}$ vector coupling and the Yukawa coupling of the top quark, respectively. The excluded parameter space is larger if all the other Wilson coefficients are assumed at their SM values. In this case, partial cancellations of BSM effects from the two operators lead to disjoint regions in the allowed parameter space. Future measurements will resolve this ambiguity with more data and by more refined binning measurements.

In Ref. [7], SM-EFT effects are tested in the $\geq 3\ell$ final states using a sophisticated MVA strategy in the 137 fb^{-1} data set from the LHC Run 2. The main processes in this category are tZq and $\mathrm{t\bar{t}Z}$ with a smaller contribution from tWZ. The five operators with the most significant effects modify the weak dipole moment interactions and the top quark's left- and right-handed vector couplings to the SM gauge bosons. An SM multi-classifier is trained on 33 event properties to discriminate between several SM processes simultaneously to improve the sensitivity. Its $\mathrm{t\bar{t}Z}$ output node is shown in Fig. 2 (left). Furthermore, eight neural network binary classifiers separate SM events from BSM events for a wide range of Wilson coefficients. The resulting exclusion contour is

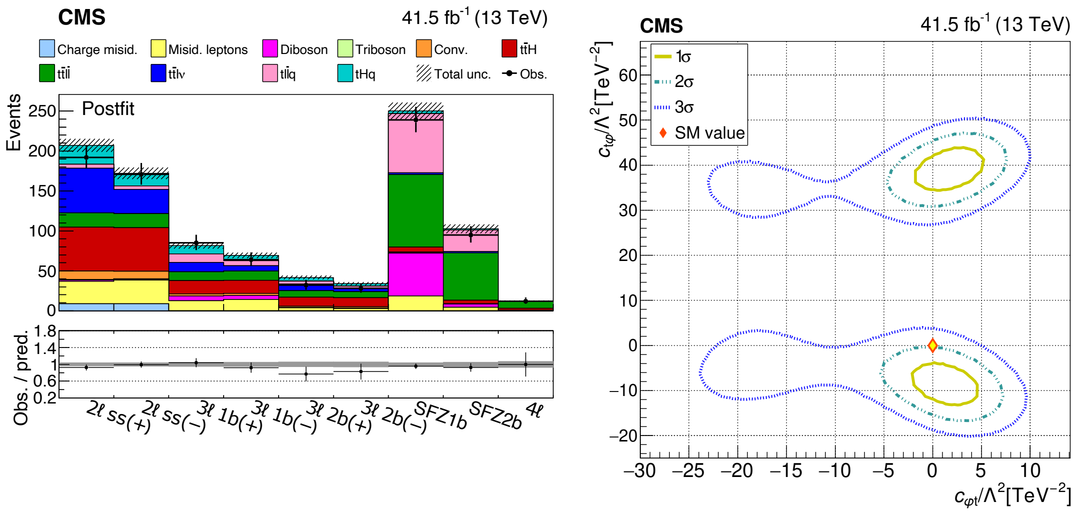

Figure 1: Expected post fit yields from performing a likelihood fit over all WCs simultaneously (left) [6]. The "Conv." refers to the photon conversion background, "Charge misid." is the lepton charge mismeasurement background, and "Misid. leptons" is the background from misidentified leptons. The jet multiplicity bins have been combined here, however, the fit is performed using all 35 event categories. The lower panel is the ratio of the observation over the prediction. The observed 1σ, 2σ, and 3σ confidence contours of a 2D scan for $C_{t\varphi}$ and $C_{\varphi t}$ with the other WCs fixed to their SM values (right). Diamond markers are shown for the SM prediction. The range on the right plot is modified to emphasize the 1σ contour.

exemplified in Fig. 2 (right) in the two-dimensional plane spanned by Wilson coefficients modifying the top quark's left- and right-handed vector couplings.

Finally, Ref. [8] reports the results of the first $\mathrm{t\bar{t}}\gamma$ cross section measurement at 13 TeV by the CMS Collaboration. Besides the inclusive and differential cross section measurements for different kinematic properties involving the photon, the single-lepton channel is used to constrain anomalous interactions of the top quark and the photon. There are 112 regions with different jet- and b-tag multiplicity, lepton flavor, and transverse photon momentum ($p_{\mathrm{T}}(\gamma)$), each potentially sensitive to SM-EFT modifications. Regions with high $p_{\mathrm{T}}(\gamma)$ are particularly sensitive to the C_{tZ} operator and allow to set the currently tightest constraints on this operator. Figure 3 shows the distribution of $p_{\mathrm{T}}(\gamma)$ in the μ channel (left), and the two-dimensional exclusion contour in the plane spanned by the real and imaginary part of the Wilson coefficient C_{tZ}. The one-dimensional limits at 95% CL are $-0.43 \le C_{\mathrm{tZ}} \le 0.38$ and $-0.43 \le C^{\mathrm{I}}_{\mathrm{tZ}} \le 0.43$

3. Summary

In this contribution, I discuss three analyses aiming at constraining various SM-EFT effects in final states with the top quark. A search for deviations in top quark final states with additional leptons constrains 15 Wilson coefficients by comparing predictions for the tZq, ttZ, tHq, and ttW on- and off the mass shell of the SM gauge bosons to data from the CMS experiment from the year 2017. An MVA-based analysis uses $\geq 3\ell$ final states and the complete Run 2 data of 137 fb^{-1} to constrain five operators modifying the weak interactions of the top quark. Finally, a differential

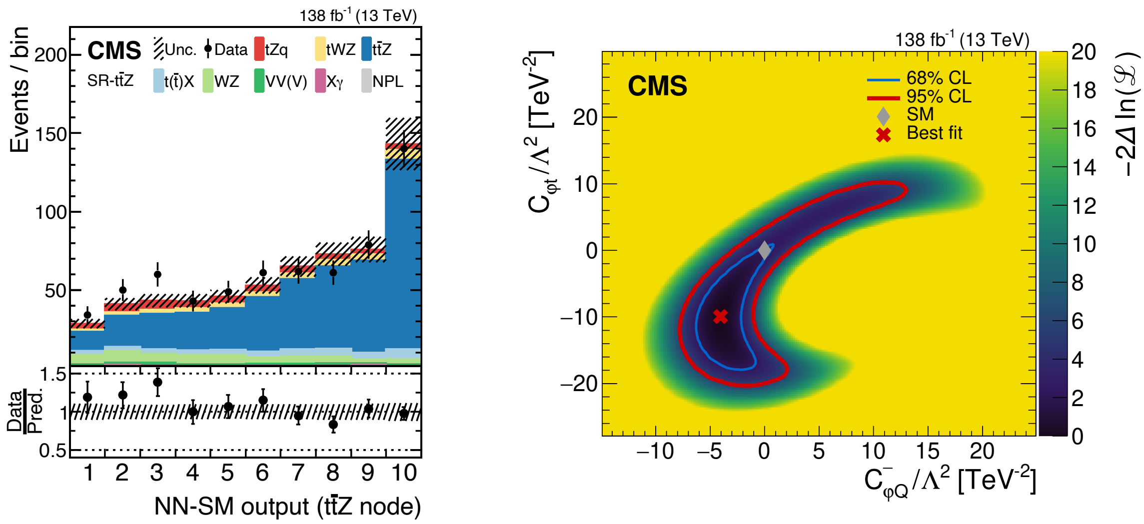

Figure 2: Pre-fit data-to-simulation comparisons for the distributions of the $t\bar{t}Z$ output node (left). The lower panel displays the ratios of the observed event yields to their predicted values. The hatched band represents the total uncertainty in the prediction. Two-dimensional scans of the negative log-likelihood as a function of $c^{-}_{\varphi Q}$ and $C_{\varphi t}$ (right), while fixing the other WCs to their SM values of zero. The thin blue line and thick red line represent the 68 and 95% CL contours, respectively.

cross section measurement of the $t\bar{t}\gamma$ process yields the strongest limit to data on the C_{tZ} Wilson coefficient, thus constraining the anomalous dipole moment interactions of the top quark.

References

[1] E. E. Jenkins, A. V. Manohar and M. Trott, JHEP **10** (2013), 087 doi:10.1007/JHEP10(2013)087, arXiv:1308.2627.

[2] R. Alonso, E. E. Jenkins, A. V. Manohar and M. Trott, JHEP **04** (2014), 159 doi:10.1007/JHEP04(2014)159, arXiv:1312.2014.

[3] E. E. Jenkins, A. V. Manohar and M. Trott, JHEP **01** (2014), 035 doi:10.1007/JHEP01(2014)035 [arXiv:1310.4838 [hep-ph]].

[4] C. Englert and M. Spannowsky, Phys. Lett. B **740** (2015), 8-15 doi:10.1016/j.physletb.2014.11.035 [arXiv:1408.5147 [hep-ph]].

[5] I. Brivio and M. Trott, Phys. Rept. **793** (2019), 1-98 doi:10.1016/j.physrep.2018.11.002 [arXiv:1706.08945 [hep-ph]].

[6] CMS Collaboration, JHEP **03** (2021), 095 doi:10.1007/JHEP03(2021)095, arXiv:2012.04120.

[7] CMS Collaboration, CMS-PAS-TOP-21-001, arXiv:2107.13896.

[8] CMS Collaboration, CMS-PAS-TOP-18-010, arXiv:2107.01508.

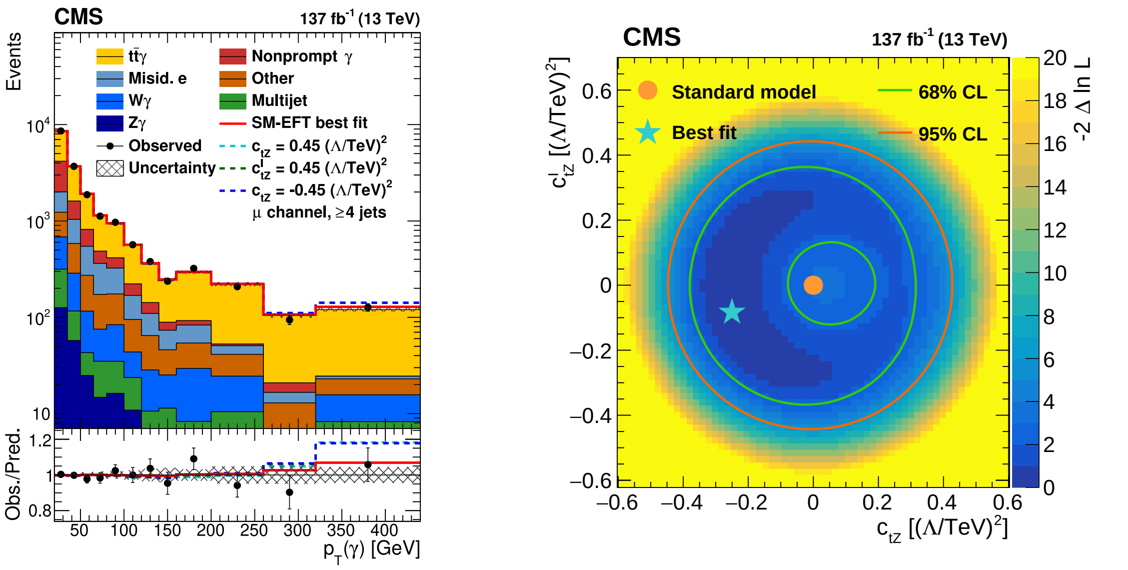

Figure 3: The observed (points) and predicted (shaded histograms) post-fit yields for the combined Run 2 data set in the $N_{\mathrm{jet}} \geq 4$ signal regions for the muon channel (left). The vertical bars on the points give the statistical uncertainties in the data. The lower panel displays the ratio of the data to the predictions, and the hatched regions show the total uncertainty. Result of the two-dimensional scan of the Wilson coefficients C_{tZ} and C^{I}_{tZ} (right). The green and orange lines indicate the 68 and 95% CL contours from the fit, respectively. The allowed areas are those between the two green contours and that inside the orange contour. The dot shows the SM prediction.